Title	Development of a hydraulic analog of the human circulatory system for testing artificial hearts : 2. design, construction and testing of the hydraulic system
Sub Title	
Author	南谷, 晴之(Minamitani, Haruyuki) Reul, Helmut Runge, Jürgen
Publisher	慶応義塾大学工学部
Publication year	1978
Jtitle	Keio engineering reports Vol.31, No.5 (1978. 2) ,p.43- 63
JaLC DOI	
Abstract	A hydraulic analog model of the human circulatory system has been developed. This model mimics the systemic and pulmonary circulations very well, each represented by a symmetrical 9-component hydraulic system corresponding to certain regions of the circulation. The input impedance spectra, phase characteristics and the input flow work rates of the model have been sufficiently approximated with physiological data. It is, thus, greatly available as a load for artificial hearts or real hearts, and also as a hydrodynamic model of the circulations.
Notes	
Genre	Departmental Bulletin Paper
URL	https://koara.lib.keio.ac.jp/xoonips/modules/xoonips/detail.php?koara_id=KO50001004-00310005-0043

KEIO ENGINEERING REPORTS
VOL. 31, NO. 5, pp. 43-63, 1978

DEVELOPMENT OF A HYDRAULIC ANALOG OF THE HUMAN CIRCULATORY SYSTEM FOR TESTING ARTIFICIAL HEARTS

2. Design, Construction and Testing of the Hydraulic System

HARUYUKI MINAMITANI

Dept. of Electrical Engineering, Keio University, Yokohama 223, Japan

HELMUT REUL and JÜRGEN RUNGE

Helmholtz Institute for Biomedical Engineering, RWTH Aachen, 5100 Aachen, West Germany

(Received May. 21, 1977)

ABSTRACT

A hydraulic analog model of the human circulatory system has been developed. This model mimics the systemic and pulmonary circulations very well, each represented by a symmetrical 9-component hydraulic system corresponding to certain regions of the circulation. The input impedance spectra, phase characteristics and the input flow work rates of the model have been sufficiently approximated with physiological data. It is, thus, greatly available as a load for artificial hearts or real hearts, and also as a hydrodynamic model of the circulations.

1. Introduction

Model experiments are generally useful in biomedical and technical investigations. It is often desired to evaluate and check the performance and function of artificial hearts and/or artificial heart valves. For the study of artificial heart, investigations in a mock circulatory system are required prior to animal experiments and clinical applications. In case that the hydraulic load is correct, a normal ejection flow behavior and a normal pattern of the pressure wave beyond the valves, comparable to pressure in the aorta or pulmonary artery, may be expected to exist. Neverthless, the proper design, construction and testing of such a system has been described very few (WESTERHOF 1971, REUL 1974/1975).

In this study, design, construction and characteristics of a hydraulic model of systemic and pulmonary circulations will be discussed and the constructed model will be tested by a way that the input impedances and flow work rates are measured, and will be compared with those of physiological data.

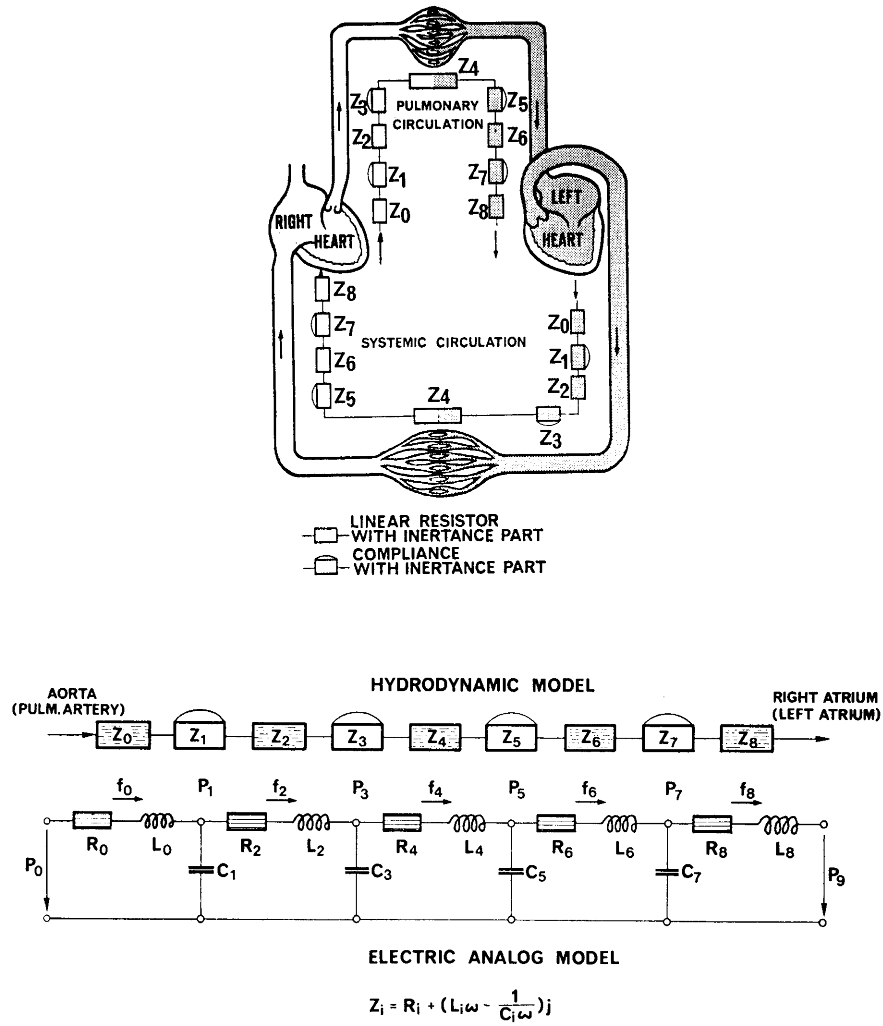

Fig. 1. Human circulatory system and its comparison with the lumped hydraulic and electrical analog models

Table 1 Set of optimum parameter values for the hydraulic model of systemic and pulmonary circulations.

Element	Systemic Circulation	Pulmonary Circulation	Dimension
R_0	0	0	dyn sec/cm^5
L_0	1.5	1.5	dyn sec^2/cm^5
C_1	$0.165 \cdot 10^{-3}$	$0.067 \cdot 10^{-3}$	cm^5/dyn
R_2	90	45	dyn sec/cm^5
L_2	1.1	1.0	dyn sec^2/cm^5
C_3	$1.1 \cdot 10^{-3}$	$2 \cdot 10^{-3}$	cm^5/dyn
R_4	1300	110	dyn sec/cm^5
L_4	3.1	2.4	dyn sec^2/cm^5
C_5	$1 \cdot 10^{-2}$	$3 \cdot 10^{-2}$	cm^5/dyn
R_6	25	25	dyn sec/cm^5
L_6	1.7	1.7	dyn sec^2/cm^5
C_7	$5 \cdot 10^{-3}$	$5 \cdot 10^{-3}$	cm^5/dyn
R_8	0	0	dyn sec/cm^5
L_8	1.1	1.1	dyn sec^2/cm^5

2. Hydraulic Model

A hydraulic analog model of the systemic and pulmonary circulations of man has been developed each by a symmetrical 9-component hydraulic system, consisting of compliances and laminar resistances with the inherent inertance parts. Fig. 1 shows a schematical figure of the model. The compliances and resistances of the model are designed according to the numerical values quoted from the former study (Reul et al. 1975, Minamitani et al. 1978) and listed in Table 1. As will be discussed later, the main problem for the transfer of theoretical data to real hydraulic elements is to keep the inertial components of the conductive tubing system and the several resistances within optimum values. This is however limited by constructive factors inherent to the design.

2.1 Design of the Hydraulic Elements

2.1.1 Resistances and Inertances

According to Wormersley (1957) and Westerhof et al. (1971), a so-called "quality factor" for a hydraulic resistor can be defined. This quality factor Q is represented by the ratio between the resistive part (R) and the inertial part (wL) of the resistor. For $Q=R/wL\ll 1$, the resistor may be considered as purely resistive and for $Q\ll 1$ as purely inductive (flow lags pressure by 90 degrees). The ideal situation would be to keep $Q\gg 1$ for the entire range of interest.

Tubes of small bores are very suitable for realization of resistors of this type, because they have a favorable ratio of resistive to inertial properties. The resistance of a tube can be described according to Poisseuille's law as:

$$R=\frac{8\mu l}{\pi r_i^4} \tag{1}$$

and its inertia as:

$$\frac{\rho l}{\pi r_i^2}=\frac{\rho l}{A} \tag{2}$$

where μ=dynamic viscosity of the fluid,
l=length of the tube,
r_i=inner radius of the tube,
ρ=density of the fluid, and
A=cross sectional area of the tube.

Hence, from equations (1) and (2) it follows,

$$\frac{R}{L}=\frac{8\nu}{r_i^2}, \quad \nu=\frac{\mu}{\rho}=\text{kinematic viscosity} \tag{3}$$

Equation (3) shows that the ratio of R/L is inversely proportional to the square of the tube radius and that the already mentioned quality factor increases with the tube radius decreasing. A further prerequisite is a linear behavior of the resistor over the entire flow range. That means, the flow must be linear and the inlet length, necessary for the development of a parabolic flow profile must be taken into account. If a nonlinearity (due to the non-parabolic entrance profile) of 10% is admitted, two governing equations for the tube length can be formulated (WESTEHOF et al. 1971):

$$l \geqq 1.14\times10^{-4}\Delta P r_i^3\rho/\mu^2 \tag{4}$$

$$l \geqq \frac{11}{64}\Delta P r_i^4\rho/\mu^2 \tag{5}$$

where ΔP=pressure difference between both sides of the tube. The tube length should be taken equal to or greater than the two resulting lengths. For pressures in the physiological range, for liquids with density and viscosity comparable to blood and for technically reasonable (danger of contamination) tube bores (0.1 mm $\leqq r_i \leqq$ 0.5 mm), only equation (5) determines the necessary minimum length.

A resistance of lower value is obtained by using N tubes in parallel. The final resistance value is then:

$$R=\frac{8\mu l}{\pi r_i^4 N} \tag{6}$$

and its inertia can be described as:

$$L=\frac{\rho l}{S} \quad \text{and} \quad S=\frac{N\pi r_0^2}{0.9}-N\pi(r_0^2-r_i^2) \tag{8}$$

Table 2a. Model resistances and inertances with the quality factors for systemic circulation

	R dyn·s/cm^5	ΔP mmHg	l mm	N	r_i mm	L dyn·s^2/cm^5	$k=1$	$k=2$	Q $k=4$	$k=6$	$k=8$	$k=10$
R_2	900	50	31.3	3040	0.32	0.29	42.5	21.2	10.6	7.1	5.3	4.25
R_4	1300	180	16.8	1420	0.17	1.12	158.4	79.2	39.6	26.4	19.8	15.8
R_6	25	10	24.2	2840	0.42	0.14	24.4	12.2	6.1	4.1	3.1	2.4

Table 2b. Model resistances and inertances with the quality factors for pulmonary circulation

	R dyn·s/cm^5	ΔP mmHg	l mm	N	r_i mm	L dyn·s^2/cm^5	$k=1$	$k=2$	Q $k=1$	$k=1$	$k=8$	$k=10$
R_2	45	10	24.2	1580	0.42	0.25	24.4	12.2	6.1	4.1	3.1	2.4
R_4	110	30	24.3	1930	0.32	0.35	42.5	21.2	10.6	7.1	5.3	4.2
R_6	25	10	24.2	2845	0.42	0.14	24.2	12.2	6.1	4.1	3.1	2.4

where N=number of the capillary tubes,
S=total cross sectional area of the in-parallel assmbled tubes (refer to Appendix)
and r_0=outer radius of the tube.

The resistors of our model are made from long, stiff and straight conduits with the peculiar radius bores. As circulatory medium in the model, the mixture liquid of glycerin, water and NaCl with a dynamic viscosity of 3.6 cpoise has been used.

The resulting data for the model resistances and inertances are listed in Table 2 together with the quality factors. The quality factor is defined here as:

$$Q=\frac{R}{w_k L} \tag{9}$$

with $w_k=2\pi k\ f_{\text{heart}}$ and $f_{\text{heart}}=1.16$ Hz. As these data show, the quality factors decreasing number of the harmonics, however they are>1 over the whole frequency range of interest.

PERIPHERAL RESISTANCE

The peripheral resistance contributes only to the input impedance for low frequencies, since the input impedance is very close to the characteristic impedance for frequencies higher than 3 Hz (BERGEL et al. 1965, GABE et al. 1964, O'ROURKE

1968, PATEL et al. 1963/1964/1965). Normal systemic mean pressure in man is about 100 mmHg. In studies on animals, however, a maximum mean pressure of twice this value may be reached. The systemic circulatory model should be therefore linear over the range from 0 to 200 mmHg for testing any type of artificial hearts and heart valves. Since the aortic resistance R_2 is 10% or less of the peripheral resistance R_4 for systemic circulation, almost this entire pressure drop (about $\Delta P=$ 180 mmHg) is over R_4 at zero and low frequencies.

The pulmonary circulatory model should be linear up to a mean pressure of 40 mmHg, and R_2 is about 25% of R_4, giving a maximum ΔP of about 30 mmHg for R_4. The choice of the length (longer or equal to the minimum length) and the given value of resistor determine the number of tubes (N) to be used in parallel (see in Table 2).

AORTIC RESISTANCE

The aortic resistances R_2 for systemic and pulmonary circulations contribute to the model over the eitire frequency range of interest. The pressure drop over these resistances at steady flow is small compared to the pressure drop over the peripheral resistance. In the systemic circulation the aortic resistance R_2 is about 10% or less of the peripheral resistance, therefore the maximum pressure drop of steady term is only about 20 mmHg. For the first harmonic of the pressure wave, however, it holds that its amplitude is about 50% of the d-c steady value of the pressure wave over the system (PATEL et al. 1965). Thus, a maximum amplitude of 100 mmHg (0.5×200 mmHg) is found for this harmonic. From the literatures (GABE et al. 1964, O'ROURKE et al. 1966/1967, PATEL et al. 1963/1964/1965) it follows that the pressure drop over the characteristic resistance R_2 at the first harmonic is about 50% of the total pressure drop over the system. Therefore a maximum pressure drop of $0.5\times100=50$ mmHg is estimated over R_2 for this harmonic. The amplitude for higher harmonics decreases, thus we may state in good approximation that the maximum pressure drop ΔP over the aortic resistance R_2 for systemic circulation is about 50 mmHg.

A similar estimation can be made for the pulmonary system and the maximum pressure drop over R_2 can be estimated as 10 mmHg (see in Table 2).

VENOUS RESISTANCE

The pressure in the venules is 10∼18 mmHg and it falls steadily in the larger veins to about 5.5 mmHg in the great veins with no pulsation. The pressure in the great veins at their entrance into the right atrium (central venous pressure) averages 4.6 mmHg but fluctuates with respiration and heart action. During inspiration the intrapleural pressure falls from -2.5 mmHg to -6 mmHg. This negative pressure is transmitted to the great veins, so that the central venous pressure fluctuates from about 6 mmHg during expiration to approximately 2 mmHg during quiet inspiration (GANONG 1973). From these considerations, however, in which the effects of muscle pump and venous pressure in head are neglected, the maximum pressure drop of 10 mmHg in the characteristic resistor of veins R_6 should be estimated for the systemic circulation.

In the left a]rium, the diastolic pressure is about 6 mmHg, and in the pulmonary capillaries non-pulsatile pressure of 10~12 mmHg can be observed. The pressure difference between the pulmonary capillaries and the left atrium is about 5 mmHg, therefore the resistor for the model of pulmonary vein may be enough to have linearity up to 10 mmHg (ΔP=10 mmHg).

INERTANCES

As mentioned, the unavoidable inertances of the hydraulic model are introduced by the connecting tubes, by the resistors which are not purely resistive, and by the four flow-probes at the in- and outlets of the model system. All inertance values represented in Table 1 include the above-listed introductory inertias, which are related to the costructive factors and calculated by the equation (2). The equation shows that the inertance is directly proportional to the length of the tube, thus the unnecessary long connecting part between the hydraulic elements must be reduced as short as possible on the design and the construction of the model.

Fig. 2 shows the integrated design of the elements Z_2, Z_3 and Z_4 for the systemic circulation. The resistors R_2 and R_4 are directly mounted into the in- and outlet of the compliance element Z_3 respectively. The resistor R_2 is on the right, R_4 on the left of the figure.

2.1.2 Compliances

For the realization of the compliances, circular silastic or natural rubber membrane have been used (manufactured by U. ADAMCZAK, Institut für Kunststoffverarbeitung, RWTH Aachen). The pressure-volume relation of these membranes is sufficiently linear within the pressure range of interest. Additional air-filled domes

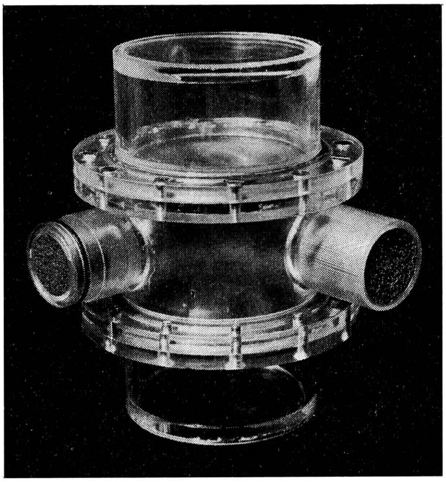

Fig. 2. Integrated design of the elements Z_2, Z_3 and Z_4 for the systemic circulation

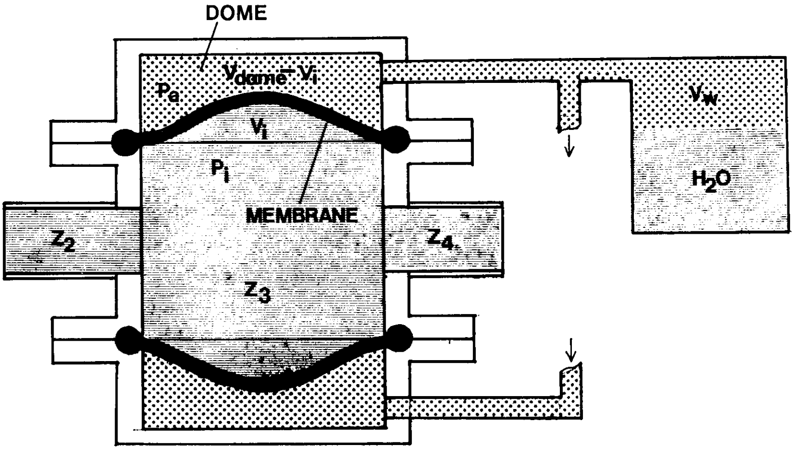

Fig. 3. Schema of a compliance element.

and air chambers allow for a variation of the total compliance in the order of 70% below the setting piont. The construction of the compliance element can be seen in Fig. 2, but the more precise representation must be done, as follows (Fig. 3): for the elastic membrane,

$$P_i - P_a = EV_i \tag{10}$$

$$V_a = V_{\mathrm{dom}} - V_i + V_w \tag{11}$$

In the air-filled dome, the following equation is given for the isothermal conditions, thus

$$P_a V_a = P_{ao} V_{ao} \tag{12}$$

Substituting equations (11) and (12) into (10),

$$P_i - P_{ao} \frac{V_{ao}}{V_a} = EV_i \tag{13}$$

$$P_i - P_{ao} \frac{V_{ao}}{V_{\mathrm{dom}} - V_i + V_w} = EV_i \tag{14}$$

For the steady condition the pressure-volume relation of this element can be then described as:

$$P_i = EV_i + \frac{P_{ao} V_{ao}}{V_{\mathrm{dom}} + V_w - V_i} \tag{15}$$

where P_i = pressure in the compliance element
P_a = pressure in the air-filled dome and the coupled air chamber
E = bulk modulus of the membrane

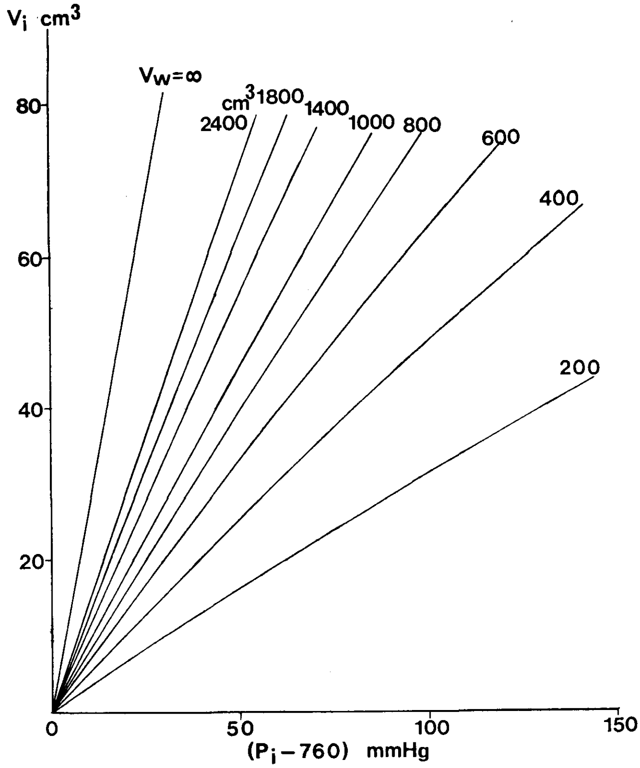

Fig. 4. Pressure-volume relation in a compliance element. Volume of air-chamber is considered as a parameter. (E=500 dyn/cm[5])

V_i = volume in the compliance element

V_a = volume of the air-filled dome and the coupled air chamber

$V_{\rm dom}$ = volume of the air-filled dome

V_w = volume of the air chamber

P_{ao} = 760 mmHg

$V_{ao} = V_a$ at P_a = 760 mmHg.

If $V_w = \infty$ or $V_{\rm dom} + V_w = \infty$,

$$P_i = EV_i + 760 \text{ mmHg} \tag{16}$$

Compliance of such a element can be defined as the ratio of pressure difference to the volume change:

$$C = \frac{\Delta V_i}{\Delta P_i} \tag{17}$$

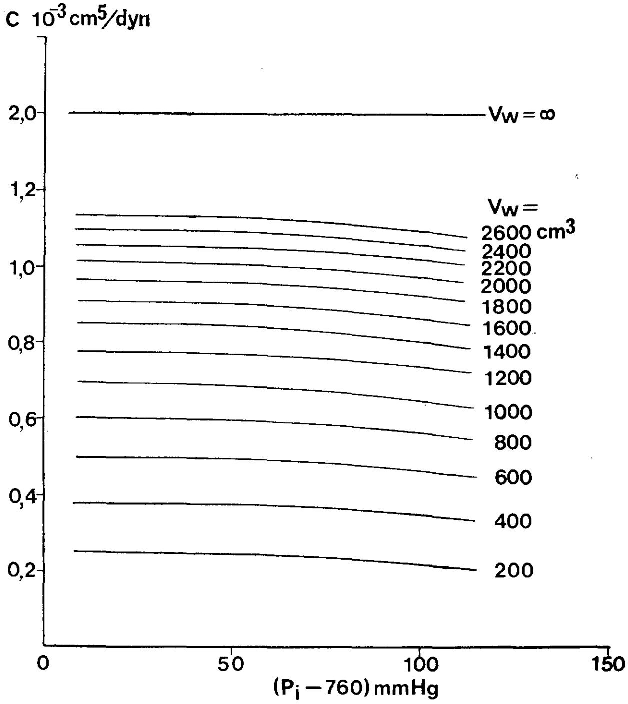

Fig. 5. Relationship between compliance and pressure in the compliance element. Volume of air-chamber is considered as a parameter. ($E = 500$ dyn/cm^5)

and its relation is depicted in Fig. 4. Fig. 5 shows the different description of Fig. 4 and it is represented that the characteristic of the compliance element gives nearly linear conformation over the pressure range of interest. When two membranes are used on both sides of the element, as thown in Fig. 2, large compliance can be realized or the dome volume and the air chamber volume can be reduced in one-half of them. To match very large compliances of the venous parts of systemic and pulmonary circulations, six membranes are used in parallel (see in Fig. 9). The compliances of both left and right atria are constructed by two silastic membranes which have proper elasticity for the atria. The cross-sectional area of the compliance elements should not be made too small so as to avoid extra mass effects. Thus, the inertia in the compliance elements might be neglected.

2.2 Construction of the Hydraulic Model

Fig. 6 gives again an aspect of the integrated assembly of elements Z_2, Z_3 and Z_4. It shows additionally the adjusting mechanism of the resistor R_4, which consists of a rotatable disc with a circular bore.

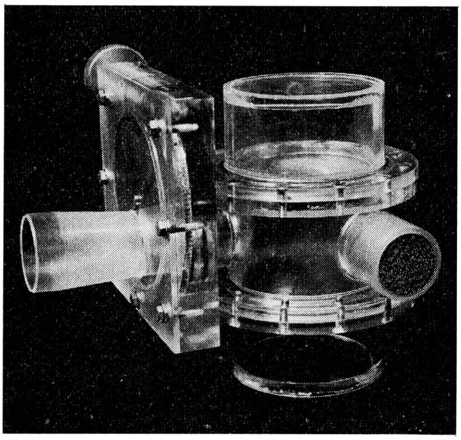

Fig. 6. Integrated assembly of the elements Z_2, Z_3 and Z_4 with the adjusting mechanism of resistance R_4.

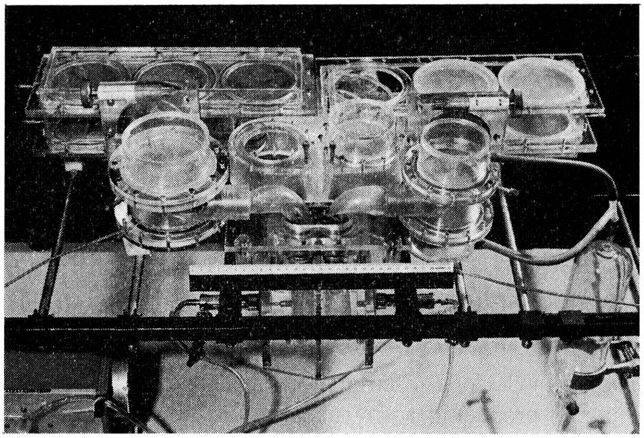

Fig. 7. Aspect of the complete hydraulic analog model.

The complete set-up for both the systemic and the pulmoarry circulation is shown Fig. 7. The systemic part lies on the right hand side, the pulmonary on the left. For better insight into the model one membrane from the systemic venous compliance are removed. It is to be seen that the crosslinked between the two circulatory systems are integrate into the venous compliance element, by using isolated channels with large cross sectional areas. The center block contains four in- and outlets of the artificial heart model, which consists of two pusher plate driven sac ventricles, and shows the built-in flow-probes and the compact arrangement of the

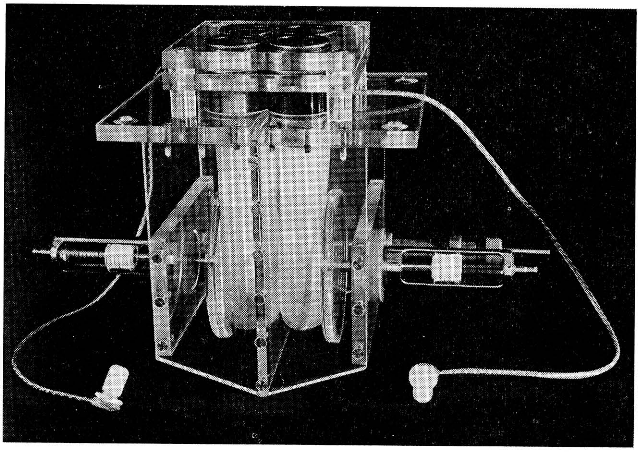

Fig. 8. A detail aspect of the artificial heart model.

atria. The two bended elastic tubes in the foreground represent the compliance elements Z_1, which are necessary for compensation of the inertia of the flow-probes. The overall dimensions of the model are $74 \times 32 \times 16$ cm. Fig. 8 gives a detail aspect of the artificial heart model, showing the pusher-plates with the coupled hydraulic high-pressure pistons on both sides and four mounted flow probes on the top.

3. Test of the Model (Characteristics of the Model)

The constructed model of the circulatory systems has been tested with the aid of a sine-wave pump, producing a sinusiodal liquid flow over a frequency range of 0.3~15 Hz. Pressure and flow at the inlet part of each system have been measured, and the input impedances for the systemic and pulmonary circulations have been calculated from the measured data. Input impedance of the circulatory system is defined as the ratio of oscillatory inlet pressure of the system to the oscillatory inlet flow as:

$$Z_k = \frac{P_k}{f_k}, \text{ and its phase } \xi_k = \varphi_k - \phi_k \tag{18}$$

where Z_k = input impedance modulus of k-th harmonic

ξ_k = phase shift between pressure and flow of k-th harmonic

P_k, φ_k = pressure modulus and phase of k-th harmonic

f_k, ϕ_k = flow modulus and phase of k-th harmonic

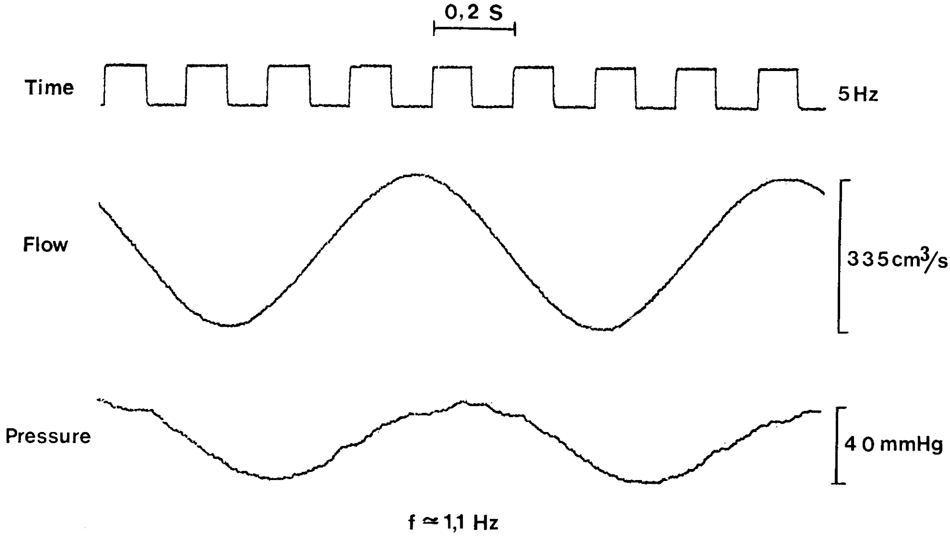

Fig. 9. Sinusoidal flow and pressure at the inlet of systemic circulation model.

Fig. 9 shows the measured sinusoidal flow f_k sin $(kwt+\phi_k)$ and the pressure change P_k sin $(kwt+\varphi_k)$ at $w=2\pi\times(1.12\text{ Hz})$. Fig. 10 shows the input impedance moduli and the phase characteristics of the constructed model with frequencies up to 8Hz. Black dots in the figure represent the measured values, and the theoretical impedances obtained from the electrical analog model (MINAMITANI et al. 1977) are described by circles. The first minimum of the impedance spectra can be found at 3.5 Hz for the systemic and also at 3.5 Hz for the pulmonary circulation. For higher frequencies, the impedance moduli do not remain nearly constrant, but slightly increase with frequency. The phase characteristic are zero for the steady term, negative for low frequencies (0.5~3 Hz) and positive for higher frequencies. Zero degree-crossings of the phase are shown at about 3.5 Hz for the systemic and pulmonary circulations respectively. It is agreed that the measured impedance moduli and phase chacteristics are about equal to those both from the electrical analog and the in-vivo measured physiological data, which are indicated by the shaded areas in the figure. But it must be pointed out here, that the impedance moduli for the systemic circulation are smaller than the theoretical ones between 2nd and 7th harmonics, and that the phase characteristic for the systemic circulation is not so well agreed with the theoretical and physiological ones between 3rd and 7th harmonics.

In this study, the experiment concerned with the combination of artificial heart and hydraulic mock circulatory system has not been carried out, but flow work rate should be estimated for good agreement of the model with physiological data. Flow work rate is represented by time-averaged product of pressure and flow for one cardiac cycle:

$$W=\frac{1}{T}\int_0^T P(t)f(t)dt \tag{19}$$

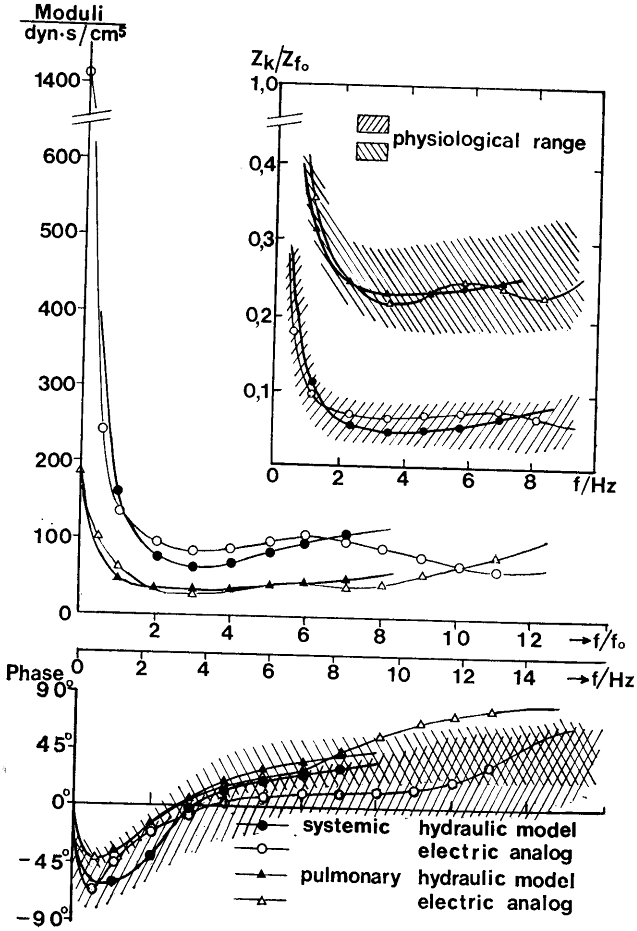

Fig. 10. Input impedance spectra and phase characteristics of the hydraulic and electrical analog model compared with physiological data.

and it is equivalent to the hydraulic power delivered to the circulatory system per unit time. Equation (19) can be simply rewritten as follows:

$$\begin{aligned} W &= W_0 + \sum_{k=1}^{m} W_k \\ &= P_0 f_0 + \frac{1}{2} \sum_{k=1}^{m} P_k f_k \cos \xi_k \\ &= \frac{P_0^2}{Z_0} + \frac{1}{2} \sum_{k=1}^{m} \frac{P_k^2}{Z_k} \cos \xi_k \end{aligned} \tag{20}$$

where P_0 = mean pressure component

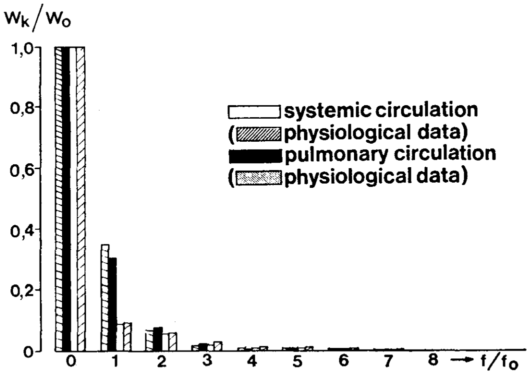

Fig. 11. Input flow work rates of the hydraulic model compared with physiological data.

f_0=steady flow component

Z_0=input impedance modulus for steady term

By quoting a desirable aortic pressure curve from the former study (REUL et al. 1975, MINAMITANI et al. 1977), the flow work rates have been calculated by equation (20) for both the systemic and pulmonary circulations. Fig. 11 shows the normalized flow work rates for each harmonic compared with the physiological data. It can be also found that the constructed hydraulic model agrees well with real circulalory systems. The pulsatile components are about 15% of the total flow work rate for the systemic and 35% for the pulmonary circulation.

4. Discussions

A lumped parameter hydraulic model of human circulatory system has been developed as a testing load for artificial hearts. This load is mainly characterized by the input impedance of the circulatory system. In this study, the input impedances and the flow work rates of the systemic and pulmonary circulations have been measured, and compared with the theoretical and the physiological ones. They represent a good agreement with the real human circulatory system, as shown by the hatched area in Fig. 10. However, the input impedance for the systemic circulation is smaller than the theoretical data over lower frequencies of 1~6 Hz. Higher input impedance moduli and higher positive phase characteristics can also be seen at higher frequencies. It is supposed that the smaller impedance at lower frequencies would be caused by the smaller values of aortic resistance R_2, the inherent inertance L_2 and aortic compliance C_3 than the desired ones. On the contrary, the higher impedance at higher frequencies would be caused by the larger inertance L_0 of the inlet part of the circulatory systems. Fig. 12 shows the result

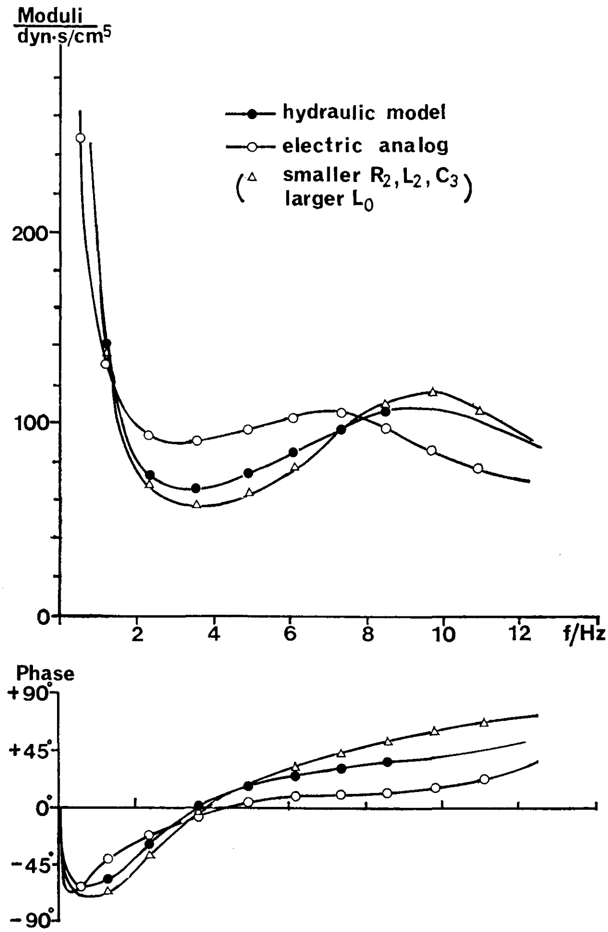

Fig. 12. Effect of different L_0, R_2, L_2 and C_3 on the input impedance for systemic circulation, estimated by electric analog model (△). Black dots represent the measured input impedance of hydraulic model, and the original theoretical values are described by circles (See in text).

obtained from an electrical analog model (MINAMITANI et al. 1977), which represents the changing of input impedance with different L_0, R_2, L_2 and C_3 for the systemic circulation (L_0=2.0 dyn·sec^2/cm^5, R_2=70 dyn·sec/cm^5, L_2=0.9 dyn·sec^2/cm^5 and C_3= 0.6 cm^5/dyn). It is obviously presumed that smaller R_2, L_2 and C_3 lead to low impedance moduli over lower frequency range of 1~6 Hz, and that larger L_0 leads to high impedance moduli and high positive phase characteristics at higher frequencies. Smaller inertance of the inlet would give an ideal characteristic for the hydraulic model, but it is mostly impossible to reduce the actual model inertance.

In Fig. 9, we can find a fluctuation superimposed on the pressure curve. This phenomenon would be caused by occurence of the turbulent flow behavior at a pressure-measuring point. The compliance C_1 of the connecting element between a flow-probe and an arterial load, as shown in Fig. 7, plays an important role for compensation of the inertia of the flow-probe. But, its long elastic tube could be considered as the source facilitating undesirable fluctuation. More precise observation for the effect of a long elastic tube on flow dynamics will be required.

This lumped model of the circulatory system has not been tested with an artificial heart or as an artificial load for a real heart, thus, the experimental observation with an artificial heart must be also carried out.

5. Conclusion

A lumped parameter hydraulic model has been developed as a testing load for artificial hearts. Each parameter of the model elements, estimated by an equivalent electrical analog model, has been realized into a compact integrated hydraulic system. This is an extended Windkessel model and it does not exhibit the phenomenon of wave travel. The input impedance spectra, phase characteristics and the flow work rates of the model have been sufficiently approximated with the physiological data.

Thus, it may be concluded that the constructed hydraulic model of the systemic and pulmonary circulations mimics a normal cardiac load very well and is greatly available as a load for artificial hearts or real hearts. It may also be useful in hydrodynamic models of the circulation.

Acknowledgement

This study has been carried out at the Helmholtz Institute for Biomedical Engineering RWTH Aachen, West Germany, and partially suported by the exchange program of RWTH Aachen and Keio University, Japan and by the A.V. Humboldt-Stiftung, West Germany. The authors express their thanks to Professors S. EFFERT M.D. and T. SUZUKI Ph. D. for the promotion of this study, and to Mr. H.P. HEIMES Dipl.-Ing. and Mr. W. TILLMAN Dipl.-Ing. for their co-operation in this research.

Appendix

In Chapter 2.1.1, the total cross sectional area of the in-parallel assembled tubes S has been estimated by equation (8):

$$S = S_R - N\pi(r_0^2 - r_j^2) = \frac{N\pi r_0^2}{0.9} - N\pi(r_0^2 - r_i^2)$$

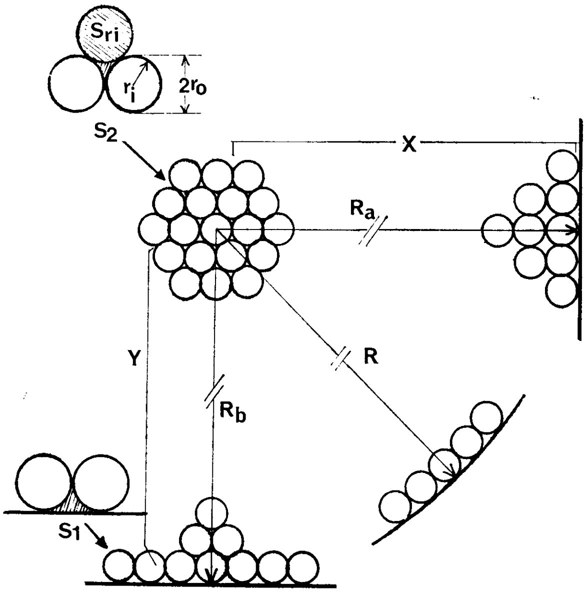

Fig 13. Sectional drawing of a resistance element.

where S_R=inner cross sectional area of a holder for the in-parallel assembled tubes. It must be checked, however, whether the above simple equation can be used for the estimation of S. From Fig. 13, the total cross sectional area S can be generally calculated as follows:

$$S = NS_{ri} + pS_1 + qS_2 \tag{21}$$

where S_{ri}=cross sectional area of a tube,

S_1=the area constructed by two circles and the wall of the holder necessary for assembling the tubes,

S_2=the area constructed by three circles,

p and q=numbers of the corresponding areas.

Since inner radius of the holder for the tubes $R \gg r_0$, and then

$$S_1 = \left(2 - \frac{\pi}{2}\right) r_0^2 \tag{22}$$

Meanwhile,

$$S_2 = \left(\sqrt{3} - \frac{\pi}{2}\right) r_0^2 \tag{23}$$

Thus,

$$S=N\pi r_i^2+p\left(2-\frac{\pi}{2}\right)r_0^2+q\left(\sqrt{3}-\frac{\pi}{2}\right)r_0^2 \tag{24}$$

where r_i = inner radius of the tube
r_0 = outer radius of the tube.

The inner cross sectional area of the holder can be also estimated by

$$S_R=N\pi r_0^2+p\left(2-\frac{\pi}{2}\right)r_0^2+q\left(\sqrt{3}-\frac{\pi}{2}\right)r_0^2 \tag{25}$$

Numbers p and q are approximated by the following equations, in which decimal fractions of both numbers are rounded.

$$p\doteqdot\frac{2\pi(R-r_0)}{2r_0}=\frac{\pi(R-r_0)}{r_0}\doteqdot\frac{\pi R}{r_0} \tag{26}$$

$$q\doteqdot\sum_{j=1}^{X}2\pi(2j-1)=2\pi X^2 \tag{27}$$

If $\pi\doteqdot3$, then $p=3R/r_0$ and $q=6X^2$
Radius R may be assumed by the following inequations (, and see Fig. 13).

$$R_b<R<R_a \tag{28}$$

in which

(a) $R_a=(2X+1)r_0$, and total number of tubes N:

$$N\doteqdot1+\frac{2\pi(2r_0)}{2r_0}+\frac{2\pi(4r_0)}{2r_0}+\cdots+\frac{2\pi(2Xr_0)}{2r_0}$$

$$=1+\pi X+\pi X^2 \tag{29}$$

Table 3. Comparison of S and S_R calculated by equations (8), (24) and (25) for systemic circulation

		X/Y	R_a/R_b	$R_b<R<R_a$	p/q	S eq. (8)/S eq. (24)	S_R eq. (8)/S_R eq. (25)
L_2	$N=3040$ $r_0=0.04$ cm $r_i=0.032$cm	31/33	$63r_0/59r_0$	$61r_0$	189/6038	11.479/11.465	16.979/16.965
L_4	$N=1420$ $r_0=025$ cm $r_i=0.017$ cm	21/23	$43r_0/41r_0$	$42r_0$	129/2771	1.600/1.602	3.098/3.101
L_6	$N=2840$ $r_0=0.05$ cm $r_i=0.042$ cm	30/32	$61r_0/57r_0$	$59r_0$	182/5655	18.213/18.209	24.780/24.776

If $\pi=3$, then $N=3X^2+3X+1,\quad X=\dfrac{-3+\sqrt{12N-3}}{6}$ (30)

(b) $R_b=(\sqrt{3}Y+3-\sqrt{3})r_0$, and total number of tubes N:

$$N \fallingdotseq 1+\frac{2\pi(\sqrt{3}Y+2-\sqrt{3})r_0}{2r_0}+\frac{2\pi(\sqrt{3}Y+2-2\sqrt{3})r_0}{2r_0}$$

$$+\cdots+2\pi$$

$$=1+\frac{\pi}{2}\{\sqrt{3}\,Y^2+(4-\sqrt{3})Y\}$$

where X and Y are columns of the assembled tubes, as described in Fig. 13.

Comparison of the total cross sectional area S calculated by equation (8) with those by equations (24) and (25) is represented below in Table 3. It gives a good approximation, hence, equations (7) and (8) can be used for estimation of the total cross sectional area S and inertia L.

REFERENCES

BERGEL, D.H. and MILNOR, W.R. (1965): Pulmonary vascular impedance in the dog, *Circulation Res.*, **16**, 401–415.

GABE, I.T., KARNELL, J., PORJÉ I.G. and RUDEWALD B. (1964): The measurement of input impedance and apparent phase velocity in the human aorta, *Acta Physiol. Scand.*, **61**, 73–85.

GANONG, W.F. (1973): *Review of Medical Physiology*, 6th Edition, **431**, Lange Medical Publications and Maruzen Co. Ltd.

MINAMITANI, H., REUL, H. and RUNGE J. (1978): Development of a hydraulic analog of the human circulatory system for testing artificial hearts—1. Parameter optimization of the hydraulic model elements, *Keio Eng. Rept.*, **31**, **4**, 27–42.

O'ROURKE, M.F. and TAYLOR, M.G. (1966): Vascular impedance of the femoral bed, *Circulation Res.*, **18**, 126–139.

O'ROURKE M.F. and TAYLOR M.G. (1967): Input impedance of the systemic circulation, *Circulation Res.*, **20**, 365–380.

O'ROURKE M.F. (1968): Impact pressure, lateral pressure and impedance in the proximal aorta and pulmonary artery, *J. Appl. Physiol.*, **25**, 533–541.

PATEL, D.J., FREITAS, F.M. and FRY D.L. (1963): Hydraulic input impedance to aorta and pulmonary artery in dogs, *J. Appl. Physiol.*, **18**, 134–140.

PATEL, D.J., AUSTEN, W.G. and GREENFIELD, J.C. (1964): Impedance of certain large blood vessels in man, *Ann. N.Y. Acad. Sci.*, **115**, 1129–1139.

PATEL, D.J., GREENFIELD J.C., AUSTEN, W.G., MORROW A.G. and FRY, D.L. (1965): Pressure-flow relationships in the ascending aorta and femoral artery of man, *J. Appl. Physiol.*, **20**, 459–463.

PATEL, D.J., MASON, D.T., ROSS, J. and BRAUNWALD, E. (1965): Harmonic analysis of pressure pulses obtained from the heart and great vessels of man, *Am. Heart J.*, **69**, 785–794.

REUL, H. and RUNGE, J. (1974): A hydraulic analog of the systemic and pulmonary circulation for testing artificial hearts (Preliminary report), *Proc. European Soc. Art. Org.*, **1**, 159-162.

REUL, H., RUNGE, J., MINAMITANI, H., and HEIMES H.P. (1975): A hydraulic load for testing artificial hearts, *Digest 15th Aniversary Int. Conf. Biol. Eng. Soc.*, 22-6.

REUL, H., MINAMITANI, H. and RUNGE, J. (1975): A hydraulic analog of the systemic and pulmonary circulation for testing artificial hearts, *Proc. European Soc. Art. Org.*, **2**, 120-127.

WESTERHOF, N., ELZINGA, G. and SIPKEMA, P. (1971): An artificial arterial system for pumping hearts, *J. Appl. Physiol.*, **31**, 776-381.

WOMERSLEY, J.R. (1957): An elastic tube theory of pulse transmission and oscillatory flow in mammalian arteries, *Wright Air Development Center, Tech. Rept.*, TR 56-614.